

LinkedNN: a neural model of linkage disequilibrium decay for recent effective population size inference

Chris C R Smith¹

¹Department of Biology, Indiana University

February 16, 2026

Abstract

Summary

A bioinformatics tool is presented for estimating recent effective population size by using a neural network to automatically compute linkage disequilibrium-related features as a function of genomic distance between polymorphisms. The new method outperforms existing deep learning and summary statistic-based approaches using relatively few sequenced individuals and variant sites, making it particularly valuable for molecular ecology applications with sparse, unphased data.

Availability and Implementation

The program is available as an easily installable Python package with documentation here: <https://pypi.org/project/linkedNN/>. The open source code is available from: <https://github.com/the-smith-lab/LinkedNN>.

Contact

Email: chriscs@iu.edu

Supplementary information

Supplementary methods and figures are available via the journal's web site.

Introduction

Linkage disequilibrium (LD) is the non-random association of alleles at different loci and is shaped by evolutionary forces including recombination and genetic drift. In particular, its magnitude reflects demographic history, where populations with larger effective size, N_e , show lower levels of LD (Hill and Robertson, 1968). This relationship has been used to develop powerful N_e estimators that leverage correlations between genotypes at different loci as a function of genomic distance (Laurie-Ahlberg and Weir, 1979; Hill, 1981; Waples, 2006; Santiago et al., 2020). LD-based approaches are especially useful for estimating *recent* N_e , because crossover events occur more frequently than mutations and can therefore shape LD patterns over shorter timescales. For example, **GONE** (Santiago et al., 2020) models the decay of LD with genomic distance to infer N_e through time, producing reasonable N_e estimates in the past 100 generations. Such LD-based methods are especially valuable in molecular ecology and conservation where unphased and relatively sparse genomic markers can nonetheless provide signal about recent N_e . Despite these advantages, summarizing genome-wide LD remains burdensome because existing approaches require analysis-specific decisions for binning SNP pairs into arbitrary, discrete distance classes. Consequently, there is a methodological need for tools that automatically extract features related to LD decay directly from polymorphism data.

Many of the deep learning architectures used to automatically extract features from SNPs are convolutional neural networks (CNNs). While CNNs have been effective for demographic inference and other tasks (Flagel et al., 2019; Torada et al., 2019; Gower et al., 2021; Sanchez et al., 2021; Wang et al., 2021; Smith et al., 2023), they have limited capacity to see LD. This issue arises in part because CNNs perform spatial operations designed for gridded, regularly spaced inputs like images, but SNPs are not uniformly distributed along chromosomes. Furthermore, the genotype information from individual sites is progressively eroded in neural network layers beyond the first convolution, making typical architectures not ideal for seeing correlations beyond adjacent SNPs in the input array. Capturing precise LD signal requires models that can represent genomic features across a continuum of genomic distances.

Here, a neural network is developed that is capable of learning LD decay-related features from SNPs as a function of genomic distance, rather than relying on grid operations to convey positional information. The method is evaluated on simulated data for estimating recent N_e , benchmarked against current CNN and summary statistic-based regression tools, and demonstrated on empirical data. The new LD layer is implemented in a bioinformatics tool called **LinkedNN** that can be used for N_e estimation or other inference tasks in diverse species.

Methods

Neural network architecture

The LD layer was implemented using PyTorch (Ansel et al., 2024) and consists of the following steps. The initial stage involves sub-sampling pairs of SNPs, as the number of possible pairs scales quadratically with the input size. Beginning with ordered polymorphisms $i = 1, \dots, M$, discretized log-uniform index jumps $\Delta_i = \text{floor}(\log\text{-U}(1, M))$ are drawn to form pairs $(i, i + \Delta_i)$, resulting in physical distances d_i within pairs that are roughly log-uniform. The number of sampled pairs is increased by repeating this process ten times, discarding pairs with $i + \Delta_i > M$, to yield a total of $P = 10M - n_{\text{skip}}$ pairs indexed by $p = 1, \dots, P$. For example, with $M = 5,000$ and ten proposed pairs per SNP, the total retained pairs is around $P \approx 44,000$. This strategy surveys a range of genomic distances without enumerating all pairs.

Features are initially extracted from the genotype inputs x_1, \dots, x_P irrespective of genomic position (Figure 1, left). Specifically, unphased genotypes are encoded as the count of the minor allele in each individual and given to a shared-weights, position-wise layer. All trainable layers have a number of output features $f = 64$ and rectified linear unit activation, except the final layer. The position-wise features in each pair are combined and given to two additional layers to compute preliminary genetic features g_p for each pair. By letting the network automatically extract features instead of manually calculating genotype correlations, it has the potential to extract non-LD features as well.

Next, the inter-SNP distances undergo further processing before being passed to any trainable layers. The d_p are transformed using radial basis functions, following the approach from Schütt et al. (2017) but applied in log space:

$$e_k(d_p) = \exp(-\gamma(\log(d_p) - \mu_k)^2)$$

where the K centers, μ_k , are log-uniformly spaced over $(1, L)$, with L being the length of the chromosome, and K is set to $\log(L)$, rounded up. The parameter γ controls the width of the radial basis functions and, in this study, is implicitly set as the spacing between adjacent centers. In effect, the feature space of the input is expanded from a single distance to a vector of features that activate depending on which center the input distance is closest to. In the present study the radial basis functions are intended to smoothly partition distances into overlapping bins, allowing the neural network to diversify what information it uses for different distance ranges. Base pair positions were used, as this approach works for non-model species lacking a genetic map, although centimorgan positions are superior and can be equivalently input to the LD layer, setting L equal to the map length.

Whereas some CNNs have used genomic positions or distances as an additional channel in the input

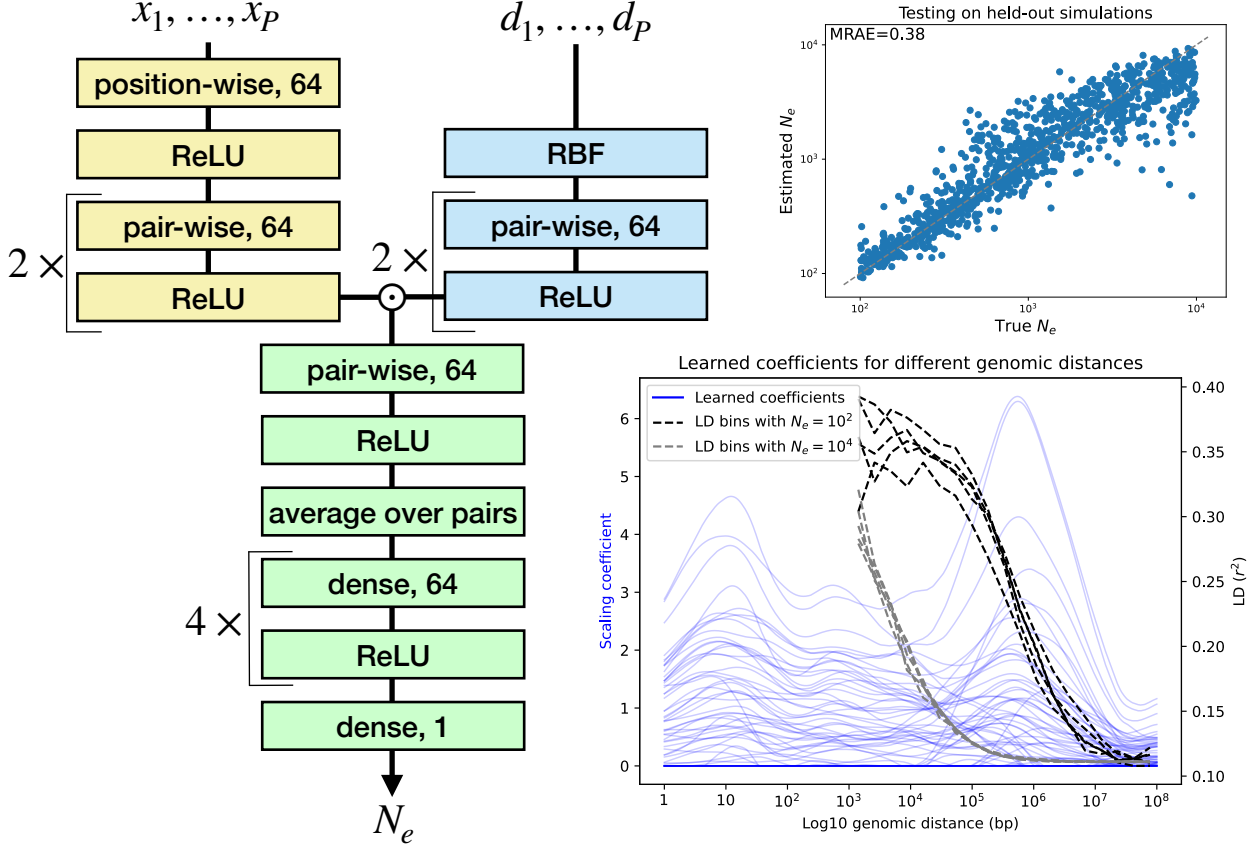


Figure 1: (Left) Neural network diagram. The inputs are genotypes for all SNP pairs x_1, \dots, x_P and corresponding genomic distances d_1, \dots, d_P . The number of filters is $f = 64$ and rectified linear unit (ReLU) activation is used on all trainable layers except the final layer. Radial basis functions (RBF) are applied to the raw distances. The output can be effective population size, N_e , or another target the user defines. (Top right). Evaluating the LD layer on 1,000 simulations held out from training. Axes are log-scale. The performance metric is mean relative absolute error (MRAE). (Bottom right). Blue lines are $f = 64$ different coefficients output by the distance-mapping network of the pre-trained LD layer for a range of genomic distance inputs, d_1, \dots, d_P , irrespective of genotypes. Larger values indicate distances the model thinks are important for scaling particular genetic features. Black and grey dashed lines are binned r^2 values calculated on SNP pairs from five $N_e = 10^2$ and five $N_e = 10^4$ simulations, respectively. Bins for distances smaller than 1,000 bp were omitted because they contain too few SNPs.

genotype array, this only permits the distance information to be conveyed additively to each filter, as the initial convolution performs a moving dot product between the input and kernel weights. To allow the distances to interact with extracted genetic features multiplicatively, the LD layer learns a set of distance coefficients specific to each SNP pair, s_p , with length equal to the number of extracted genotype features, f . The s_p generating network consists of two layers applied to the radial basis features from each SNP pair. These coefficients are used to directly rescale the corresponding genotype features from each SNP pair, elementwise: $g'_p = g_p \odot s_p$. As a result, certain genotype features from some SNP pairs are amplified if their distance is relevant to the inference, or silenced if their distance is less pertinent. This spatial

mapping network addresses a similar need as the continuous filter convolution from Schütt et al. (2017) or edge-conditioned filters from Simonovsky and Komodakis (2017), as the learned features are conditioned by a learned function of distance between data points. However, instead of message-passing between nodes as with graph convolutions, the LD layer focuses on the interactions between nodes (SNP pairs), and uses fewer trainable parameters. A similar approach was used by Smith et al. (2024) to rescale genotype features based on two-dimensional geographic distances between individuals.

After scaling by genomic distance, the g'_m are each input to an additional layer, and then averaged across all SNP pairs. This averaging is inspired by the approach of Hill (1981) for combining data from all SNP pairs. Last, the averaged features are input to a regression head consisting of five additional dense layers for estimating N_e . The number of trainable weights in the LD layer is relatively small compared to a typical CNN, although training is slower due to computing many SNP pairs. Training uses simulated datasets that match a focal empirical dataset in terms of sample size and other parameters. In particular, a reference genome and recombination rate estimate or genetic map are required for the method. Additional details are available in the Supplementary Material.

Results

Model evaluation

The LD layer was compared with existing methods for estimating three parameters in a two-epoch demographic history, using 1,000 held-out simulations with $n = 10$ sampled individuals and $M = 5,000$ SNPs. The best performing model was the LD layer, predicting the recent N_e parameter with mean relative absolute error (MRAE) of 0.380 (Figure 1, top right). Second, the pairwise-CNN architecture from Smith and Kern (2023) gave MRAE=0.422 for the recent N_e parameter. Next, summary statistic-based regression using a neural network or random forest gave MRAE=0.429 and MRAE=0.456, respectively. Finally, applying a basic CNN produced an MRAE of 0.511; relative to the basic CNN, the LD layer improved the MRAE by 25.6%.

Interpreting learned distance-coefficients

Next, the spatial coefficients, s_p , computed by the trained LD layer were examined for an array of input distances (Figure 1, bottom right). This inspection showed that the model learns unique coefficients corresponding to each genetic feature, with some coefficients displaying strong heterogeneity across the range of distances; this contrasts with the coefficients formed with random weight initializations which show no

structure (Figure S1). In particular, 16 out of 64 coefficients had maximum values between 5×10^5 and 5×10^6 bp, indicating this was an important range of inter-SNP distances for the current analysis. This distance is also larger than the mean spacing between consecutive SNPs in the input array of approximately 2×10^4 , suggesting it is helpful to convey more distant SNP pairs than what the first layer of a CNN with kernel size of 2 would see. In addition, the 5×10^5 to 5×10^6 bp sweet spot falls near the inflection point of the simulated LD-decay curve in small- N_e simulations (Figure 1), suggesting the genetic features associated with these coefficients are related to LD. Fifteen coefficients had maximum values between 50 and 5×10^5 bp, which may capture LD-related features at various stages of decay in larger populations, or correspond to genetic features unassociated with LD, e.g., measures of genetic variation. From the remaining, nine features were canceled out by coefficients with flat values at zero, and 24 coefficients had maximum values between 5 and 50 bp; as SNP pairs rarely fell into the latter range, a likely explanation for these peaks is recognition of individual training examples, i.e., overfitting.

Empirical application

Last, the LD layer was evaluated on publicly available data from harbor porpoises (*Phocoena phocoena*) (Celemín et al., 2025), using 5,000 SNPs from the largest contig (maximum distance 6.7×10^7 bp) in $n = 10$ genotypes from the Belt Sea group. Uncertainty was assessed using 100 predictions, drawing random SNPs with non-missing data within the subsample each repetition. The estimated recent N_e under the two-epoch model was 1,411 (ranging from 1,119 to 1,659 among repetitions), with a population size change occurring 42.1 (28.8, 53.2) generations ago, and older N_e of 5,921 (5,273, 6,867). The inferred time parameter corresponds to 501.0 years in the past, applying a generation time of 11.9 years (Celemín et al., 2025). These estimates seem reasonable, given the analyzed specimens were sampled geographically intermediate between the critically endangered Proper Baltic Sea sub-population (Carlström et al., 2023) and the Atlantic where larger populations exist (Celemín et al., 2025). The inferred N_e was smaller than that estimated by Celemín et al. (2025) using a sequentially Markovian coalescent-based method (Terhorst et al., 2017) which may struggle to estimate very recent demographic history.

Discussion

The new layer automatically computes LD-related features as a function of genomic distance between SNPs for estimating effective population size. Evaluated on simulations, the LD layer was more accurate than machine learning-based regression models using mainstream summary statistics and CNN-based models. While the inclusion of ideal summary statistics, such as carefully tuned LD-decay bins, might narrow this

performance gap, the LD layer bypasses such an analysis by automatically learning which inter-SNP distances are useful. The new method performs well with $n = 10$ individuals and 5,000 variants, making it valuable for molecular ecology applications with sparse, unphased SNPs, for example, from reduced representation sequencing. However, the usefulness of LD-information will depend strongly on the analyzed demographic history and the number of recombination events between analyzed SNPs. Future research may diversify the set of features extracted from SNPs by combining the LD layer with other architectures, which might help estimate complex demographic histories.

References

Jason Ansel, Edward Yang, Horace He, Natalia Gimelshein, Animesh Jain, Michael Voznesensky, Bin Bao, Peter Bell, David Berard, Evgeni Burovski, et al. Pytorch 2: Faster machine learning through dynamic python bytecode transformation and graph compilation. In *Proceedings of the 29th ACM International Conference on Architectural Support for Programming Languages and Operating Systems, Volume 2*, pages 929–947, 2024.

J Carlström, I Carlén, M Dähne, PS Hammond, S Koschinski, K Owen, S Sveegaard, and R Tiedemann. *Phocoena phocoena* (baltic sea subpopulation). the iucn red list of threatened species 2023: e. t17031a50370773, 2023.

Enrique Celemín, Marijke Autenrieth, Anna Roos, Iwona Pawliczka, Maria Quintela, Ulf Lindstrøm, Harald Benke, Ursula Siebert, Christina Lockyer, Per Berggren, et al. Evolutionary history and seascape genomics of harbour porpoises (*phocoena phocoena*) across environmental gradients in the north atlantic and adjacent waters. *Molecular Ecology Resources*, 25(5):e13860, 2025.

Lex Flagel, Yaniv Brandvain, and Daniel R Schrider. The unreasonable effectiveness of convolutional neural networks in population genetic inference. *Molecular biology and evolution*, 36(2):220–238, 2019.

Graham Gower, Pablo Iáñez Picazo, Matteo Fumagalli, and Fernando Racimo. Detecting adaptive introgression in human evolution using convolutional neural networks. *Elife*, 10:e64669, 2021.

WG Hill and Alan Robertson. Linkage disequilibrium in finite populations. *Theoretical and applied genetics*, 38(6):226–231, 1968.

William G Hill. Estimation of effective population size from data on linkage disequilibrium1. *Genetics Research*, 38(3):209–216, 1981.

CC Laurie-Ahlberg and BS Weir. Allozymic variation and linkage disequilibrium in some laboratory populations of *drosophila melanogaster*. *Genetics*, 92(4):1295–1314, 1979.

Alistair Miles, Murillo F Rodrigues, Peter Ralph, Jerome Kelleher, Max Schelker, Rahul Pisupati, Summer Rae, Tim Millar, et al. *cggh/scikit-allel*: v1. 3.13. *Zenodo*, 2021.

F. Pedregosa, G. Varoquaux, A. Gramfort, V. Michel, B. Thirion, O. Grisel, M. Blondel, P. Prettenhofer, R. Weiss, V. Dubourg, J. Vanderplas, A. Passos, D. Cournapeau, M. Brucher, M. Perrot, and E. Duchesnay. Scikit-learn: Machine learning in Python. *Journal of Machine Learning Research*, 12:2825–2830, 2011.

Alan R Rogers and Chad Huff. Linkage disequilibrium between loci with unknown phase. *Genetics*, 182(3):839–844, 2009.

Théophile Sanchez, Jean Cury, Guillaume Charpiat, and Flora Jay. Deep learning for population size history inference: Design, comparison and combination with approximate bayesian computation. *Molecular Ecology Resources*, 21(8):2645–2660, 2021.

Enrique Santiago, Irene Novo, Antonio F Pardiñas, María Saura, Jinliang Wang, and Armando Caballero. Recent demographic history inferred by high-resolution analysis of linkage disequilibrium. *Molecular Biology and Evolution*, 37(12):3642–3653, 2020.

Kristof Schütt, Pieter-Jan Kindermans, Huziel Enoc Sauceda Felix, Stefan Chmiela, Alexandre Tkatchenko, and Klaus-Robert Müller. Schnet: A continuous-filter convolutional neural network for modeling quantum interactions. *Advances in neural information processing systems*, 30, 2017.

Martin Simonovsky and Nikos Komodakis. Dynamic edge-conditioned filters in convolutional neural networks on graphs. In *Proceedings of the IEEE conference on computer vision and pattern recognition*, pages 3693–3702, 2017.

Chris CR Smith and Andrew D Kern. dispersenn2: a neural network for estimating dispersal distance from georeferenced polymorphism data. *BMC bioinformatics*, 24(1):385, 2023.

Chris CR Smith, Silas Tittes, Peter L Ralph, and Andrew D Kern. Dispersal inference from population genetic variation using a convolutional neural network. *Genetics*, 224(2):iyad068, 2023.

Chris CR Smith, Gilia Patterson, Peter L Ralph, and Andrew D Kern. Estimation of spatial demographic maps from polymorphism data using a neural network. *Molecular Ecology Resources*, 24(7):e14005, 2024.

Jonathan Terhorst, John A Kamm, and Yun S Song. Robust and scalable inference of population history from hundreds of unphased whole genomes. *Nature genetics*, 49(2):303–309, 2017.

Luis Torada, Lucrezia Lorenzon, Alice Beddis, Ulas Isildak, Linda Pattini, Sara Mathieson, and Matteo Fumagalli. Imagene: a convolutional neural network to quantify natural selection from genomic data. *BMC bioinformatics*, 20(Suppl 9):337, 2019.

Zhanpeng Wang, Jiaping Wang, Michael Kourakos, Nhung Hoang, Hyong Hark Lee, Iain Mathieson, and Sara Mathieson. Automatic inference of demographic parameters using generative adversarial networks. *Molecular ecology resources*, 21(8):2689–2705, 2021.

Robin S Waples. A bias correction for estimates of effective population size based on linkage disequilibrium at unlinked gene loci. *Conservation Genetics*, 7(2):167–184, 2006.

Supplementary material

Model evaluation framework

Simulations for training and evaluation were implemented in `msprime` with sample size of $n = 10$ diploid individuals. A two-epoch demographic scenario was used with ancestral size N_a drawn from $\log\text{-U}(10^2, 10^4)$, a population size change at time $T_1 = \log\text{-U}(10, 10^3)$ generations in the past, and recent size $N_1 = \log\text{-U}(10^2, 10^4)$. Mutations were incrementally added to each simulated tree sequence until a fixed number of $M = 5,000$ SNPs was achieved; this strategy prevents the model from using the number of segregating sites, which in many datasets reflects sequencing depth rather than evolutionary processes. The vector including all three z -score-normalized parameters was used as the target for training several models including: (i) the LD layer, (ii) a basic CNN, (iii) a pairwise-CNN, and summary statistic-based regression with (iv) a random forest and (v) a neural network. The size of the training set was 50,000 simulations—80% for training, 20% for hyperparameter tuning—and 1,000 simulations were held out for testing.

Training the LD layer and CNN-based models used batches of 100 training examples, mean squared error loss, the Adam optimizer, and starting learning rate of 1×10^{-4} . The learning rate was halved every ten training iterations without reduction in validation loss.

Choice of CNN-based models

The basic CNN from Smith et al. (2023) was selected from among the several available CNN architectures because it is tuned for smaller SNP datasets, but this model is otherwise similar to that of (Flagel et al., 2019). The pairwise-CNN is a relatively new architecture from Smith and Kern (2023) that was originally built for spatial applications but has not been benchmarked for estimating recent N_e . Equivalent training

settings—batch size, optimizer, etc.—were used with each CNN-based model for direct comparison with the LD layer.

Summary statistic-based regression

The following summary statistics were calculated for each simulated dataset with `scikit-allel` (Miles et al., 2021):

- mean, across SNPs, of the average number of pairwise differences between chromosomes
- variance of the mean number of pairwise differences among SNPs
- mean Tajima’s D among non-overlapping 100-SNP windows
- variance of mean Tajima’s D among windows
- mean observed rate of heterozygosity among SNPs
- variance of the observed rate of heterozygosity among SNPs
- mean expected rate of heterozygosity among SNPs
- variance of the expected rate of heterozygosity among SNPs
- mean inbreeding coefficient among SNPs
- variance of the inbreeding coefficient among SNPs
- mean LD among pairs of variants calculated as r from Rogers and Huff (2009)
- variance in LD among pairs of variants
- each element of the folded allele frequency spectrum (ten bins for $n = 10$ diploids)

Each summary statistic was z -score normalized (for the neural network). The random forest and neural network regressors from `scikit-learn` (Pedregosa et al., 2011) were each trained with default settings on the same 50,000 simulations used to train the CNN-based and LD models, and tested on the same 1,000 held-out simulations.

Parameter	Model	RMSE	r^2	MRAE
N_1	CNN	1587.8	0.795	0.511
	summary statistics + random forest	1480.2	0.838	0.456
	summary statistics + neural network	1450.9	0.847	0.429
	pairwise-CNN	1507.4	0.842	0.422
	LD layer	1472.7	0.86	0.38
T_1	CNN	166.5	0.581	0.749
	summary statistics + random forest	191.4	0.561	0.760
	summary statistics + neural network	193.8	0.567	0.687
	pairwise-CNN	171.6	0.63	0.682
	LD layer	150.5	0.671	0.578
N_a	CNN	611.2	0.972	0.172
	summary statistics + random forest	1160.9	0.915	0.319
	summary statistics + neural network	1154.9	0.920	0.314
	pairwise-CNN	513.2	0.981	0.131
	LD layer	485.3	0.986	0.121

Table S1: Model evaluation results. RMSE = root mean squared error, calculated on un-normalized outputs. The r^2 statistic was calculated on log-transformed outputs. MRAE = mean relative absolute error, calculated on un-normalized outputs.

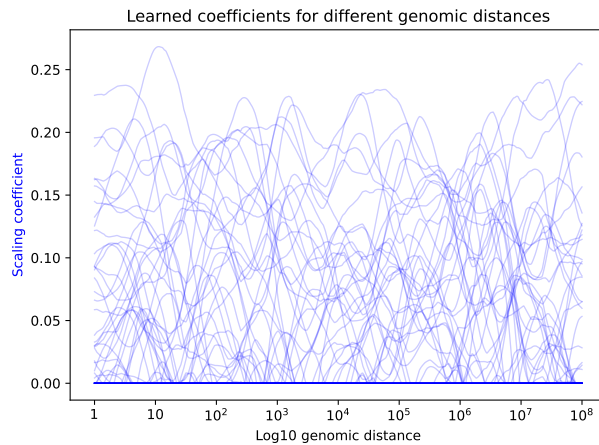


Figure S1: Blue lines are $f = 64$ different coefficients output by the distance-mapping network at initialization—without training—for a range of distance inputs.